Selective Lysis of Bacteria but Not Mammalian Cells by Diastereomers of Melittin: Structure−Function Study†

Ziv Oren and Yechiel Shai*

Department of Membrane Research and Biophysics, Weizmann Institute of Science, Rehovot, 76100 Israel

Received October 7, 1996; Revised Manuscript Received November 26, 1996⊗

ABSTRACT: Studies on lipid−peptide interactions of cytolytic polypeptides tend to emphasize the importance of the amphipathic α-helical structure for their cytolytic activity. In this study, diasetereomers of the bee venom melittin (26 a.a.), a non-cell-selective cytolysin, were synthesized and investigated for their structure and cytolytic activity toward bacteria and mammalian cells. Similarly to the findings with the diastereomers of the less cytolytic peptide pardaxin (33 a.a.) (Shai & Oren, 1996), the melittin diastereomers lost their α-helical structure, which abrogated their hemolytic activity toward human erythrocytes. However, they retained their antibacterial activity and completely lysed both Gram-positive and Gram-negative bacteria, as revealed by transmission electron microscopy. To understand the molecular mechanism underlying this selectivity, binding experiments utilizing the intrinsic tryptophan of melittin, tryptophan quenching experiments using brominated phospholipids, and membrane destabilization studies were done. The data revealed that the melittin diastereomers bound to and destabilized only negatively-charged phospholipid vesicles, in contrast to native melittin, which binds strongly to both negatively-charged and zwitterionic phospholipids. However, the partition coefficient, the depth of penetration into the membrane, and the membrane-permeating activity of the diastereomers with negatively-charged phospholipids were similar to those obtained with melittin. The results obtained do not support the formation of transmembrane pores as the mode of action of the diastereomers, but rather suggest that these peptides bind to the surface of the bacterial membrane, cover it in a "carpet-like" manner, and dissolve it like a detergent. The results presented here together with those obtained with the cytolytic peptide pardaxin suggest that the combination of hydrophobicity and net positive charge may be sufficient in the design of potent diastereomers of antibacterial polypeptides for the treatment of infectious diseases.

Studies on lipid−peptide interactions of cytolytic polypeptides tend to emphasize the importance of the amphipathic α-helical structure for their cytolytic activity. This conclusion is based mainly on studies with cytolysins that act on either mammalian cells or bacteria alone or on both types of cells. A major group of cytolytic peptides in this family are host-defense short linear polypeptides (≤40 a.a.), which are devoid of disulfide bridges (Boman, 1995). These polypeptides vary considerably in chain length, hydrophobicity, and overall distribution of charges, but share a common structure upon association with lipid bilayers, namely, an amphipathic α-helix structure (Segrest et al., 1990). The list includes: (i) cytolysins that are toxic for bacteria only; e.g., cecropins, isolated from the cecropia moth (Steiner et al., 1981), magainins (Zasloff, 1987), and dermaseptins (Mor et al., 1991) isolated from the skin of frogs; (ii) cytolysins that are selectively cytotoxic to mammalian cells, such as, δ-hemolysin isolated from *Staphylococcus aureus* (Dhople & Nagaraj, 1993); and (iii) cytolysins that are not cell selective, such as the bee venom melittin (Habermann & Jentsch, 1967) and the neurotoxin pardaxin (Lazarovici et al., 1986; Shai et al., 1988). Despite extensive studies, the exact mode of action of short linear cytotoxic polypeptides is not known yet, and it is not clear whether similar structural features are required for their cytotoxicity toward mammalian cells and bacteria.

Melittin, a 26-residue amphipathic polypeptide, is the major component of the venom of the honey bee *Apis mellifera* (Habermann & Jentsch, 1967) and is one of the most studied membrane-seeking polypeptides (Dempsey, 1990). Melittin is highly cytotoxic for mammalian cells, but is also a highly potent antibacterial agent (Blondelle & Houghten, 1991; Steiner et al., 1981; Wade et al., 1992). Numerous studies have been undertaken to determine the nature of the interaction of melittin with membranes, both with the aim of understanding the molecular mechanism of melittin-induced hemolysis and as a model for studying the general features of structures of membrane proteins and interactions of such proteins with phospholipid membranes. Much of the currently described evidence indicates that different molecular mechanisms may underlie different actions of melittin. Nevertheless, the amphipathic α-helical structure has been shown to be prerequisite for its various activities (Blondelle & Houghten, 1991; Perez et al., 1994, 1995; Weaver et al., 1992).

The structure of melittin has been investigated using various techniques. The results of X-ray crystallography and NMR in methanolic solutions indicate that the molecule consists of two α-helical segments (residues 1−10 and 13−26) that intersect at an angle of 120°. These segments are connected by a hinge (11−12) to form a bent α-helical rod with the hydrophilic and hydrophobic sides facing opposite

† This research was supported by the Israel Academy of Sciences and Humanities and by the Pasteur-Weizmann Research Foundation.

* To whom correspondence should be addressed, at the Department of Membrane Research and Biophysics, The Weizmann Institute of Science, Rehovot, 76100 Israel. Tel: 972-8-9342711; Fax: 972-8-9344112; E-mail: bmshai@weizmann.weizmann.ac.il.

⊗ Abstract published in *Advance ACS Abstracts,* January 15, 1997.

S0006-2960(96)02507-X CCC: $14.00

directions. Four such monomeric melittin molecules cluster together, through hydrophobic interactions, to form a tetramer (Anderson et al., 1980; Bazzo et al., 1988; Terwilliger & Eisenberg, 1982a,b). Upon initial interaction with membrane surfaces, it has been found that the tetramer dissociates to monomers, which retain α-helical conformations prior to insertion into the membrane (Altenbach & Hubbell, 1988; Batenburg & de Kruijff, 1988; Hider et al., 1983).

Melittin shares some similarities with pardaxin, a marine cytolytic polypeptide isolated from the Moses sole fish, *Pardachirus marmoratus* (Lazarovici et al., 1986; Shai et al., 1988). Both pardaxin and melittin are composed of two helices with a proline hinge between them. Furthermore, they exhibit significant homology in their N-helices, which are mostly hydrophobic (Thompson et al., 1986). However, pardaxin (net charge +1) contains an additional seven amino acids at its C-terminal side with a charge of −2, while melittin (net charge +6) terminates with an amide group and contains the positively-charged tetrapeptide sequence Lys-Arg-Lys-Arg. There are several functional differences between pardaxin and melittin. Pardaxin binds similarly to both zwitterionic and negatively-charged phospholipids (Rapaport et al., 1996; Rapaport & Shai, 1991), while melittin binds better to negatively-charged than to zwitterionic phospholipids (Batenburg et al., 1987a−c; Dufourcq & Faucon, 1977). Also, pardaxin binds to phospholipids with positive cooperativity (Rapaport et al., 1996; Rapaport & Shai, 1991) while melittin binds with negative cooperativity (Batenburg et al., 1987a−c; Dufourcq & Faucon, 1977). Although both pardaxin and melittin are potent antibacterial peptides against Gram-positive and Gram-negative bacteria, pardaxin is 40−100-fold less hemolytic than melittin toward human erythrocytes (Oren & Shai, 1996).

In a previous study, diastereomers (D-amino acid containing analogues) of pardaxin were synthesized and then structurally and functionally investigated (Shai & Oren, 1996). The diastereomers did not retain their α-helical structure, which caused abrogation of their cytotoxic effects on mammalian cells. However, they retained a high antibacterial activity, which was expressed by complete lysis of both Gram-positive and Gram-negative bacteria. Thus, the α-helical structure of pardaxin was shown to be important for cytotoxicity against mammalian cells, but not to be a prerequisite for antibacterial activity. However, in another study, a single D-amino acid incorporated into the non-hemolytic antibacterial peptide magainin abolished almost totally its antibacterial activity (Chen et al., 1988).

Whether loss of the α-helical structure can preserve antibacterial activity and abolish cytotoxicity toward mammalian cells in other non-cell-selective cytolysins, and to understand the molecular mechanism underlying this selectivity, we synthesized diastereomers of melittin and determined their structure, mode of action with phospholipid membranes, and cytotoxicity against bacteria and human erythrocytes.

The data reveal that, similarly to the diastereomers of pardaxin, the diastereomers of melittin lost their α-helical structure, which caused a loss in their hemolytic, but not in their antibacterial, activity. Furthermore, binding to membranes, tryptophan-quenching, and membrane destabilization studies demonstrated that although the melittin diastereomers did not bind and destabilize zwitterionic phospholipid vesicles, they could do so with negatively-charged phospholipid vesicles, and in a fashion similar to that of wild-type melittin. Correlations between structural components of melittin and its diastereomers and their cytotoxic action are discussed.

EXPERIMENTAL PROCEDURES

Materials. Butyloxycarbonyl-(amino acid)-(phenylacetamido) methyl resin was purchased from Applied Biosystems (Foster City, CA), and butyloxycarbonyl (Boc) amino acids were obtained from Peninsula Laboratories (Belmont, CA). Other reagents used for peptide synthesis included trifluoroacetic acid (TFA;[1] Sigma), *N*,*N*-diisopropylethylamine (DIEA, Aldrich, distilled over ninhydrin), dicyclohexylcarbodiimide (DCC, Fluka), 1-hydroxybenzotriazole (HOBT, Pierce), and dimethylformamide (peptide synthesis grade, Biolab). Egg phosphatidylcholine (PC) and phosphatidylserine (PS) from bovine spinal cord (sodium salt, grade I) were purchased from Lipid Products (South Nutfield, U.K). Cholesterol (extra pure) was supplied by Merck (Darmstadt, Germany) and recrystallized twice from ethanol. 3,3′-Diethylthiodicarbocyanine iodide [diS-C_2-5] was obtained from Molecular Probes (Eugene, OR). Native melittin was purchased from Sigma. Commercially available melittin usually contains traces of phospholipase A_2, which causes rapid hydrolysis of phospholipids. Therefore, special care was taken to remove all the phospholipase A_2 from melittin using RP-HPLC. All other reagents were of analytical grade. Buffers were prepared in double glass-distilled water.

Peptide Synthesis and Purification. Peptides were synthesized by a solid phase method on butyloxycarbonyl-(amino acid)-(phenylacetamido) methyl resin (0.05 mequiv) (Merrifield et al., 1982). The resin-bound peptides were cleaved from the resins by hydrogen fluoride (HF), and after HF evaporation extracted with dry ether. These crude peptide preparations contained one major peak, as revealed by RP-HPLC, that was 50−70% pure peptide by weight. The synthesized peptides were further purified by RP-HPLC on a C_{18} reverse phase Bio-Rad semipreparative column (300 Å pore size). The column was eluted in 40 min, using a linear gradient of 25−80% acetonitrile in water, both containing 0.05% TFA (v/v), at a flow rate of 1.8 mL/min. The purified peptides, which were shown to be homogeneous (∼95%) by analytical HPLC, were subjected to amino acid analysis and to mass spectrometry to confirm their sequences.

Transamidation of the Peptides. Resin-bound peptide (20 mg) was treated for 3 days with a mixture composed of 1:1 v/v of saturated ammonia solution (30%) in methanol and DMSO (1:1 v/v) which resulted in transamidation of the carboxylate group of the glutamine residue located at the C-terminus of [D]-$V^{5,8}$,I^{17},K^{21}-melittin. Thus, peptides were obtained in which all the protecting groups remained attached, but whose C-terminal residues were modified by one amide group. The methanol and ammonia were evapo-

[1] Abbreviations: CD, circular dichroism; CFU, colony-forming units; DMF, dimethylformamide; DMSO, dimethyl sulfoxide; diS-C_2-5, 3,3′-diethylthiodicarbocyanine iodode; HEPES, *N*-(2-hydroxyethyl)piperazine-*N*′-2-ethanesulfonic acid; HF, hydrogen fluoride; hRBC, human red blood cells; MIC, minimal inhibitory concentration; Pam, (phenylacetamido)methyl; PBS, phosphate buffered saline; PC, egg phosphatidylcholine; PS, phosphatidylserine; PTA, phosphotungstic acid; RP-HPLC, reverse phase high-performance liquid chromatography; SUV, small unilamellar vesicles; TFA, trifluoroacetic acid; TFE, 2,2,2-trifluoroethanol.

rated under a stream of nitrogen, and the protected peptides were extracted from the resin with DMSO and precipitated with dry ether. The products were then subjected to HF cleavage and to further purification using RP-HPLC as described above.

Preparation of Liposomes. Small unilamellar vesicles (SUV) were prepared by sonication of PC/cholesterol (10:1 w/w) or PC/PS (1:1 w/w) dispersions. Briefly, dry lipid and cholesterol (10:1 w/w) were dissolved in a $CHCl_3$/MeOH mixture (2:1 v/v). The solvents were then evaporated under a stream of nitrogen, and the lipids (at a concentration of 7.2 mg/mL) were subjected to a vacuum for 1 h and then resuspended in the appropriate buffer, by vortexing. The resultant lipid dispersions were then sonicated for 5−15 min in a bath type sonicator (G1125SP1 sonicator, Laboratory Supplies Co. Inc., Hicksville, NY) until clear. The lipid concentrations of the resulting preparations were determined by phosphorus analysis (Bartlett, 1959). Vesicles were visualized using a JEOL JEM 100B electron microscope (Japan Electron Optics Laboratory Co., Tokyo, Japan) as follows. A drop of vesicles was deposited on a carbon-coated grid and negatively stained with uranyl acetate. Examination of the grids demonstrated that the vesicles were unilamellar with an average diameter of 20−50 nm (Papahadjopoulos & Miller, 1967).

CD Spectroscopy. The CD spectra of the peptides were measured with a Jasco J-500A spectropolarimeter after calibrating the instrument with (+)-10-camphorsulfonic acid. The spectra were scanned at 23 °C in a capped, quartz optical cell with a 0.5 mm path length. Spectra were obtained at wavelengths of 250−190 nm. Eight scans were taken for each peptide at a scan rate of 20 nm/min. The peptides were scanned at concentrations of 1.5×10^{-5}−2.0×10^{-5} M in 40% trifluoroethanol (TFE). Fractional helicities (Greenfield & Fasman, 1969; Wu et al., 1981) were calculated as follows:

$$f_h = \frac{[\theta]_{222} - [\theta]^0_{222}}{[\theta]^{100}_{222} - [\theta]^0_{222}} \quad (1)$$

where $[\theta]_{222}$ is the experimentally-observed mean residue ellipticity at 222 nm, and the values for $[\theta]^0_{222}$ and $[\theta]^{100}_{222}$, which correspond to 0% and 100% helix content at 222 nm, are estimated to be 2000 and 32 000 deg·cm^2/dmol, respectively (Wu et al., 1981).

Antibacterial Activity of Melittin and Its Diastereomers. The antibacterial activity of native melittin and its diastereomers was examined in sterile 96-well plates (Nunc F96 microtiter plates) in a final volume of 100 μL as follows. Aliquots (50 μL) of a suspension containing bacteria at a concentration of 10^6 colony-forming units (CFU)/mL in culture medium (LB medium) were added to 50 μL of water containing the peptide in serial 2-fold dilutions in water. Inhibition of growth was determined by measuring the absorbance at 492 nm with a Microplate autoreader El309 (Bio-tek Instruments), after an incubation of 18−20 h at 37 °C. Antibacterial activities were expressed as the minimal inhibitory concentration (MIC), the concentration at which 100% inhibition of growth was observed after 18−20 h of incubation. The bacteria used were: *Escherichia coli* D21, *Acinetobacter calcoaceticus* Ac11, *Bacillus megaterium* Bm11, and *Bacillus subtilis* ATCC 6051.

Hemolysis of Human Red Blood Cells. The peptides were tested for their hemolytic activities against human red blood cells (hRBC). Fresh hRBC with EDTA were rinsed 3 times with PBS (35 mM phosphate buffer/0.15 M NaCl, pH 7.3) by centrifugation for 10 min at 800g and resuspended in PBS. Peptides dissolved in PBS were then added to 50 μL of a solution of the stock hRBC in PBS to reach a final volume of 100 μL (final erythrocyte concentration, 5% v/v). The resulting suspension was incubated under agitation for 30 min at 37 °C. The samples were then centrifuged at 800*g* for 10 min. Release of hemoglobin was monitored by measuring the absorbance of the supernatant at 540 nm. Controls for zero hemolysis (blank) and 100% hemolysis consisted of hRBC suspended in PBS and Triton 1%, respectively.

Visualization of the Effects of the Peptides on Bacteria by Electron Microscopy. Samples containing *E. coli* (10^6 CFU/mL) in LB medium were incubated with the various peptides at their MIC, and one dilution less than the MIC, for 16 h, and then centrifuged for 10 min at 3000*g*. The pellets were resuspended, and a drop containing the bacteria was deposited onto a carbon-coated grid which was then negatively-stained with 2% phosphotungstic acid (PTA), pH 6.8. The grids were examined using a JEOL JEM 100B electron microscope.

Membrane Permeation Induced by the Peptides. Membrane permeation was assessed utilizing the diffusion potential assay (Loew et al., 1983; Sims et al., 1974) as previously described (Shai et al., 1990, 1991). In a typical experiment, in a glass tube, 4 μL of a liposomes suspension (final phospholipids concentration of 33 μM), in a K^+ containing buffer (50 mM K_2SO_4, 25 mM HEPES-SO_4^{2-}, pH 6.8), was diluted in 1 mL of an isotonic K^+ free buffer (50 mM Na_2SO_4, 25 mM HEPES-SO_4^{2-}, pH 6.8), and the fluorescent, potential-sensitive dye diS-C_2-5 was then added. Valinomycin (1 μL of 10^{-7} M) was added to the suspension in order to slowly create a negative diffusion potential inside the vesicles, which led to a quenching of the dye's fluorescence. Once the fluorescence had stabilized, which took 3−10 min, peptides were added. The subsequent dissipation of the diffusion potential, as reflected by an increase in fluorescence, was monitored on a Perkin Elmer LS-50B spectrofluorometer, with the excitation set at 620 nm, the emission at 670 nm, and the gain adjusted to 100%. The percentage of fluorescence recovery, F_t, was defined as:

$$F_t = [(I_t - I_0)/(I_f - I_0)] \times 100 \quad (2)$$

where I_0 = the initial fluorescence, I_f = the total fluorescence observed before the addition of valinomycin, and I_t = the fluorescence observed after adding the peptide at time *t*.

Binding of Peptides to Vesicles. The interaction of [D]-$V^{5,8}$,I^{17},K^{21}-melittin with vesicles consisting of zwitterionic (PC) or negatively-charged phospholipids (PC/PS) was characterized by measuring changes in the emission intensity of the peptides' intrinsic tryptophan in SUV titration experiments. Briefly, SUV were added to a fixed amount of peptide (0.5 μM) dissolved in buffer containing 50 mM Na_2SO_4, 25 mM HEPES-SO_4^{2-}, pH 6.8, at 24 °C. A 1-cm path length quartz cuvette that contained a final reaction volume of 2 mL was used in all experiments. The fluorescence intensity was measured as a function of the lipid/peptide molar ratio (4 separate experiments) on a Perkin-Elmer LS-5 spectrofluorometer, with excitation set at 280 nm, using a 5 nm slit, and emission set at 340 nm, using a 2.5 nm slit.

Table 1: Sequences and Designations of Melittin and its Diastereomers

Peptide designation	Sequence [a]
melittin [b]	GIGAVLKVLTTGLPALISWIKRKRQQ-NH_2
[D]-$V^{5,8}$,I^{17},K^{21}-melittin	GIGA**V**LK**V**LTTGLPAL**I**SWI**K**RKRQQ-NH_2
[D]-$V^{5,8}$,I^{17},K^{21}-melittin-COOH	GIGA**V**LK**V**LTTGLPAL**I**SWI**K**RKRQQ-COOH

[a] Bold and underlined amino acids were substituted with their D-enantiomers. [b] Underlined sequences designate the N- and C-helices, respectively.

The binding isotherms were analyzed as a partition equilibrium, using the following formula:

$$X_b = K_P C_f \quad (3)$$

where X_b is defined as the molar ratio of bound peptide (C_b) per total lipid (C_L), K_P corresponds to the partition coefficient, and C_f represents the equilibrium concentration of the free peptide in solution. For practical purposes, it was assumed that the peptides initially were partitioned only over the outer leaflet (60%) of the SUV. Therefore, the partition equation becomes:

$$X_b^* = K_P^* C_f \quad (4)$$

where X_b* is defined as the molar ratio of bound peptide per 60% of total lipid, and K_P* is the estimated surface partition constant. The curve resulting from plotting X_b* vs free peptide, C_f, is referred to as the conventional binding isotherm.

Tryptophan Quenching Experiments. Tryptophan which is sensitive to its environment has been utilized previously in combination with brominated phospholipids (Br-PC) to evaluate peptide localization in the membrane (Bolen & Holloway, 1990; De Kroon et al., 1990). Br-PC employed as quenchers of tryptophan fluorescence are suitable for probing the membrane insertion of peptides, since they act over a short distance and do not drastically perturb the membrane. Melittin and its diastereomer, each of which contains one tryptophan residue, were added (final concentration of 0.5 μM) to 2 mL of buffer (50 mM Na_2SO_4, 25 mM HEPES-SO_4^{2-}, pH 6.8) containing 20 μL (50 μM) of Br-PC/PS (1:1 w/w) SUV, thus establishing a lipid/peptide ratio of 100:1. After a 2 min incubation at room temperature, an emission spectrum of the tryptophan was recorded using a Perkin-Elmer LS-50B spectrofluorometer, with excitation set at 280 nm (8 nm slit). SUV composed of PC/PS (1:1 w/w) and which contained 25% of either 6,7 Br-PC,or 9,10 Br-PC, or 11,12 Br-PC, were used. Three separate experiments were conducted for each peptide. In control experiments, PC/PS (1:1 w/w) SUV without Br-PC were used.

RESULTS

In order to further examine the role of the α-helical structure of cytolysins in their cytotoxicity against mammalian cells and bacteria and to gain insight into the mechanism underlying this effect, two diastereomers of melittin were synthesized. The peptides were then characterized with regard to their structure, biological function, and interaction with bacteria and model membranes composed of either zwitterionic or negatively-charged phospholipids. The list of the peptides and their designations is given in Table 1. The list includes: native melittin, and [D]-$V^{5,8}$,I^{17},K^{21}-melittin in which four D-amino acids were incorporated along its N- and C-helices (the C-terminus was either amidated or left as a free carboxylate).

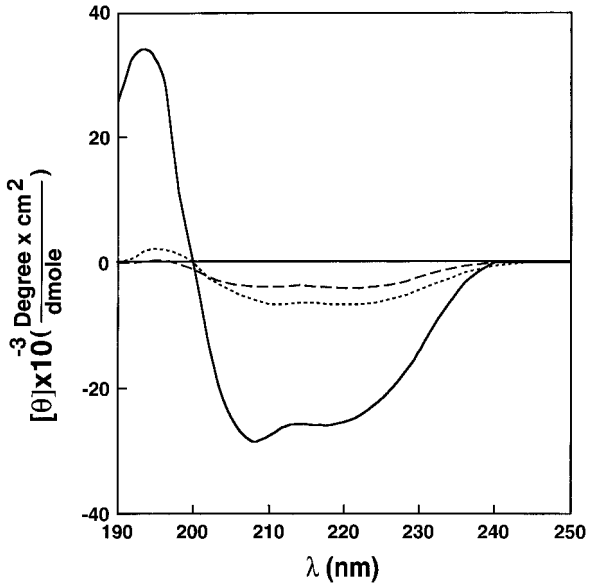

FIGURE 1: CD spectra of melittin and melittin diastereomers. Spectra were taken at peptide concentrations of $(0.8-2.0) \times 10^{-5}$ M in 40% TFE/water. melittin, (—); [D]-$V^{5,8}$,I^{17},K^{21}-melittin (···); [D]-$V^{5,8}$,I^{17},K^{21}-melittin-COOH (– –).

CD Spectroscopy. The extent of the α-helical structure of the peptides was determined from their CD spectra in 40% TFE, a solvent that strongly promotes α-helical structure. As expected, the α-helical content of the diastereomers was much lower (80% decrease) than that of melittin, as reflected by the minima at 208 and 222 nm (Figure 1). The α-helix content of melittin was 73% compared to 15% and 7% in its diastereomers, [D]-$V^{5,8}$,I^{17},K^{21}-melittin and [D]-$V^{5,8}$,I^{17},K^{21}-melittin-COOH, respectively.

Antibacterial and Hemolytic Activity of the Peptides. The hemolytic activity of the peptides against the highly susceptible human erythrocytes and their potential to inhibit the growth of different species of bacteria were investigated. The antibiotic tetracycline served as a control in the antibacterial assay. A dose response curve for the hemolytic activity of the peptides was obtained (Figure 2). Table 2 gives the MIC for a representative set of test bacteria, which includes two Gram-negative species (*Escherichia coli* and *Acinetobacter calcoaceticus*) and two Gram-positive species (*Bacillus megaterium* and *Bacillus subtilis*). The introduction of D-amino acids into melittin dramatically reduced its hemolytic activity, which paralleled the loss of the α-helical content in the corresponding analogues. Melittin, with the highest α-helical content, was the most potent, while up to the maximum concentration tested (50 μM), [D]-$V^{5,8}$,I^{17},K^{21}-

Table 2: Minimal Inhibitory Concentration (μM) of Melittin and Its Diastereomers. Results are the mean of three independent experiments, each performed in duplicate, with a standard deviation of 20%

peptide designation	minimal inhibitory concentration (μM)			
	E. coli (D21)	*A. calcoaceticus* (Ac11)	*B. megaterium* (Bm11)	*B. subtilis* (ATCC 6051)
melittin	5	20	0.3	0.4
[D]-$V^{5,8}$,I^{17},K^{21}-melittin	12	12	0.8	3.5
[D]-$V^{5,8}$,I^{17},K^{21}-melittin-COOH	20	20	1.5	8
dermaseptin-S	6	3	0.5	4
tetracycline	1.5	1.5	1.2	6.5

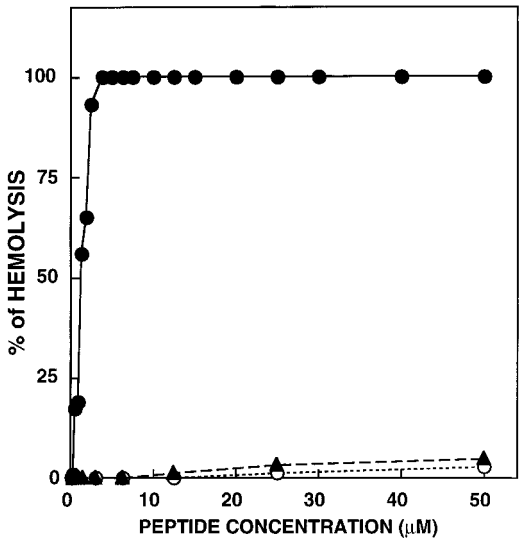

FIGURE 2: Dose−response of the hemolytic activity of the peptides toward hRBC. The assay was performed as described in the Experimental Procedures section. Designations are as follows: filled circles, melittin; empty circles, [D]-$V^{5,8}$,I^{17},K^{21}-melittin-COOH; filled triangles, [D]-$V^{5,8}$,I^{17},K^{21}-melittin.

melittin and [D]-$V^{5,8}$,I^{17},K^{21}-melittin-COOH, with the lowest α-helical content, were practically devoid of hemolytic activity. However, despite the dramatic decrease in the hemolytic activity of the diastereomers, they both retained most of the potent antibacterial activity of the parent peptide. Furthermore, the antibacterial activity of [D]-$V^{5,8}$,I^{17},K^{21}-melittin-COOH was only slightly lower than that of [D]-$V^{5,8}$,I^{17},K^{21}-melittin, which indicates that the amide group at the C-terminus of melittin does not contribute significantly to the antibacterial activity. In contrast, cecropin with a free carboxylic C-terminal had a significant lower antibacterial activity than that of the native cecropin with an amidated C-terminal (Li et al., 1988).

Electron Microscopy Study of Bacterial Lysis. The effect of the [D]-$V^{5,8}$,I^{17},K^{21}-melittin on the morphology of intact and treated bacteria was visualized using transmission electron microscopy. At the MIC, the peptide caused total lysis of the bacteria (Figure 3C). However, at concentrations lower then the MIC, patches were observed on the bacterial wall (Figure 3B). These patches might represent an initial step in the lytic process.

Mode of Interaction with Phospholipid Membranes. Since the biological activities of [D]-$V^{5,8}$,I^{17},K^{21}-melittin and [D]-$V^{5,8}$,I^{17},K^{21}-melittin-COOH were similar, only the mode of interaction of [D]-$V^{5,8}$,I^{17},K^{21}-melittin with model phospholipid membranes was compared to that of melittin, in order to elucidate the basis of the membrane selectivity observed. For that purpose, we measured the ability of the peptides to dissipate the diffusion potential created in both PC and PC/PS vesicles, determined the partition coefficients

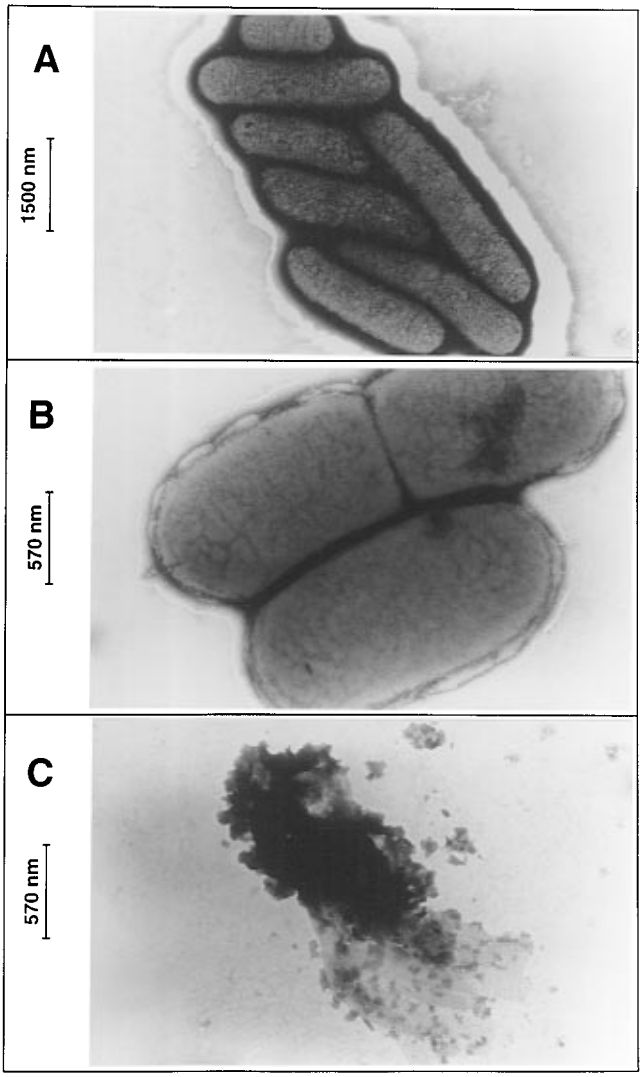

FIGURE 3: Electron micrographs of negatively-stained *E. coli* untreated and treated with [D]-$V^{5,8}$,I^{17},K^{21}-melittin. Panel A: Control. Panel B: After treatment of the bacteria with the peptide at a concentration lower than the MIC. Panel C: After treatment of the bacteria with the peptide at the MIC concentration.

of the peptides with both types of vesicles, and determined the localization of the peptide when bound to membranes.

Membrane Permeability Induced by the Peptides. Various concentrations of melittin and [D]-$V^{5,8}$,I^{17},K^{21}-melittin were mixed with vesicles that had been pretreated with the fluorescent dye, diS-C_2-5, and valinomycin. The kinetics of the fluorescence recovery was monitored with time, and the maximum level reached as a function of peptide concentration was determined (Figure 4). Both peptides had similar membrane-permeating activity with PC/PS vesicles, which demonstrated that introduction of D-amino acids into melittin does not affect the ability of the resulting diastere-

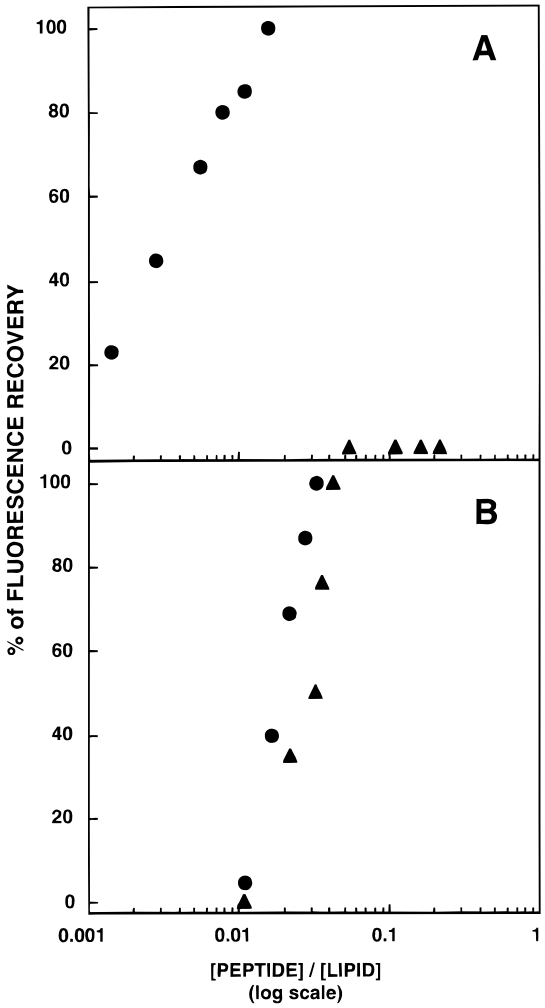

FIGURE 4: Maximal dissipation of the diffusion potential in vesicles, induced by the peptides. The peptides were added to isotonic K^+ free buffer containing SUV composed of PC (panel A) or PC/PS (panel B), pre-equilibrated with the fluorescent dye diS-C_2-5 and valinomycin. Fluorescence recovery was measured 10−20 min after the peptides were mixed with the vesicles. Filled circles, melittin; filled triangles, [D]-$V^{5,8}$,I^{17},K^{21}-melittin.

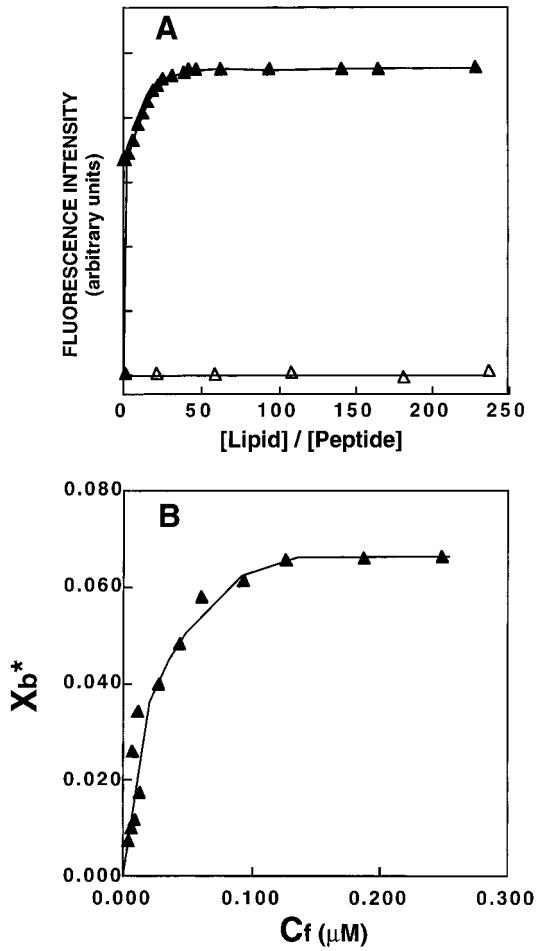

FIGURE 5: Panel A: Increase in the fluorescence of [D]-$V^{5,8}$,I^{17},K^{21}-melittin (0.5 μM total concentration) upon titration with PC/PS vesicles (filled triangles) or PC vesicles (empty triangles), with excitation wavelength set at 280 nm and emission at 340 nm. The experiment was performed at 25 °C in 50 mM Na_2SO_4, 25 mM HEPES-SO_4^{2-}, pH 6.8. Panel B: Binding isotherm derived from panel A by plotting X_b* (molar ratio of bound peptide per 60% of lipid) versus C_f (equilibrium concentration of free peptide in the solution).

omer to permeate negatively-charged phospholipid (PS/PC) membranes. However, while melittin was also highly active with PC vesicles, the diastereomer was totally devoid of membrane-permeating activity with PC vesicles (up to the maximal concentration tested).

Binding Studies. The inability of the diastereomer to permeate PC vesicles may be due to its inability to bind to PC, or alternatively, it may bind to PC vesicles, but once bound cannot organize into structures that induce membrane leakage. In order to differentiate between these two possibilities, a binding study was conducted. The single Trp residue at position 19 of [D]-$V^{5,8}$,I^{17},K^{21}-melittin was used as an intrinsic fluorescence probe to follow its binding to PC and PC/PS vesicles. A fixed concentration (~0.5 μM) of the peptide was titrated with the desired vesicles (PC or PC/PS), and an increase in the fluorescence intensity was observed if binding occurred. Plotting of the resulting increases in the fluorescence intensities of Trp as a function of lipid:peptide molar ratios yielded conventional binding curves (Figure 5A). The binding curve of [D]-$V^{5,8}$,I^{17},K^{21}-melittin with PC/PS reveals that almost all the peptide molecules bound to the vesicles at a lipid:peptide molar ratio of 100:1. However, with PC vesicles a net increase in the fluorescence of the Trp was not observed even with the maximal lipid:peptide molar ratio tested, which indicated that the peptide does not bind to PC vesicles. Binding isotherms were constructed by plotting X_b* (the molar ratio of bound peptide per 60% of the total lipid) versus C_f (the equilibrium concentration of the free peptide in the solution) (Figure 5B). The surface partition coefficients were estimated by extrapolating the initial slopes of the curves to C_f values of zero. The estimated surface partition coefficient, K_P*, of [D]-$V^{5,8}$,I^{17},K^{21}-melittin was $(1.1 \pm 0.2) \times 10^4$ M^{-1} (obtained from 4 measurements). This value is similar to the value reported for melittin binding to phosphatidylglycerol/phosphatidylcholine $(4.5 \pm 0.6) \times 10^4$ M^{-1} (Beschiaschvili & Seelig, 1990)].

The shape of the binding isotherm of a peptide can provide information on the organization of the peptide within membranes (Schwarz et al., 1987). The binding isotherm of [D]-$V^{5,8}$,I^{17},K^{21}-melittin bends downward, indicating a negative cooperativity. A possible explanation for this negative cooperativity is that, at low concentration, [D]-$V^{5,8}$,I^{17},K^{21}-melittin binding to PS/PC is enhanced by the negative charge of the phospholipid headgroups compared to the partition equilibrium with no charge effect. In

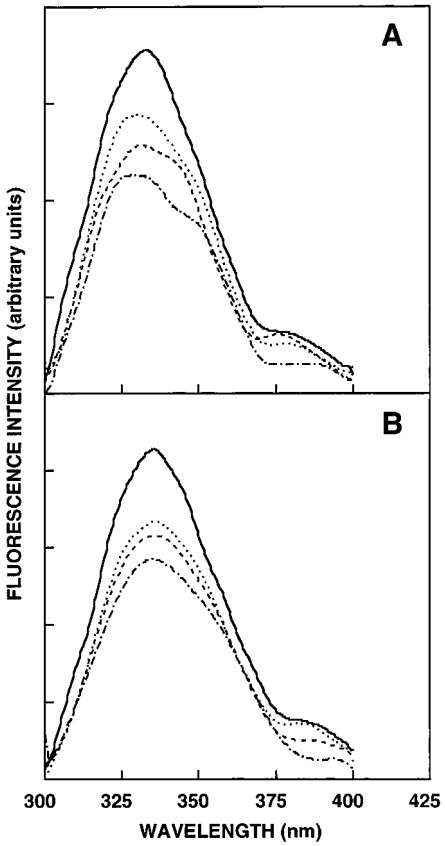

FIGURE 6: Quenching of the environmentally-sensitive tryptophan by brominated phospholipids. Melittin (panel A) and [D]-$V^{5,8}$,I^{17},K^{21}-melittin (panel B) were added to buffer containing PC/PS (1:1 w/w) SUV. The SUV contained 25% of either 6,7-Br-PC (—•—), 9,10-Br-PC (- - -), or 11,12-Br-PC (•••). After 2 min incubation, an emission spectrum of the tryptophan was recorded using a spectrofluorometer with excitation set at 280 nm. For comparison, PC/PS (1:1 w/w) SUV with no Br-PC were used (—).

addition, upon binding to the membrane the peptide partially neutralizes the negative membrane surface charge. However, once the membrane surface charge is neutralized, further [D]-$V^{5,8}$,I^{17},K^{21}-melittin binding is difficult, since repulsion of like charges becomes the dominant factor. Similar results were obtained in studies of melittin binding to negatively-charged phospholipid membranes (Batenburg et al., 1988, 1987a−c; Beschiaschvili & Seelig, 1990). Interestingly, unlike melittin which binds strongly also to PC vesicles (Dufourcq & Faucon, 1977; Kuchinka & Seelig, 1989), [D]-$V^{5,8}$,I^{17},K^{21}-melittin did not bind to PC vesicles.

Tryptophan Quenching Experiments. A tryptophan residue naturally present in the sequence of a protein or a peptide can serve as an intrinsic probe for the localization of the peptide within a membrane. Melittin contains a tryptophan residue at position 19, the N-terminal side of the C-helix. With both melittin and [D]-$V^{5,8}$,I^{17},K^{21}-melittin, the largest quenching of tryptophan fluorescence was observed with 6,7-Br-PC/PS vesicles (Figure 6). Less quenching was observed with 9,10-Br-PC/PS, and the least with 11,12-Br-PC/PS. These results indicate that, upon binding to vesicles, the peptides were located near the headgroups of the phospholipids.

DISCUSSION

Numerous studies led to the conclusion that an amphipathic α-helix is a prerequisite structure for the activity of most linear lytic peptides. One of the most studied peptides within this family is the bee venom melittin. In solution, melittin contains four regions: the N-terminal α-helix (a.a. 1−9), the flexible "hinge" region (a.a. 10−12), the central α-helix (a.a. 13−20), and the C-terminal positively-charged region (a.a. 21−26) (Anderson et al., 1980; Bazzo et al., 1988; Terwilliger & Eisenberg, 1982a,b). In this study, D-amino acids were incorporated into the N- and C-terminal helices in a manner that would cause the largest disruption to these helices. Indeed, the incorporation of D-amino acids into melittin dramatically reduced its α-helical structure (Figure 1). Interestingly, some low residual α-helix structure still remained, which can be attributed to the limited effect of a single D-amino acid on the α-helical structure (Rothemund et al., 1995).

The disruption of the α-helical structure totally abolished the hemolytic activity of the analogues (Figure 2), thus indicating the importance of this structure for the cytotoxicity of the peptide against erythrocytes. However, the diastereomers still exhibited high antibacterial activity (Table 2), which suggests that the amphipathic α-helical structure is not crucial for antibacterial activity. Similar results were obtained with the cytotoxicity of pardaxin diastereomers (Shai & Oren, 1996), even though pardaxin and melittin do not act similarly on phospholipid membranes.

The interaction of melittin and its diastereomer with model phospholipid membranes was examined in order to elucidate the basis of the selective lytic ability of the diastereomers against bacteria. In many studies on the binding of melittin to phospholipids of various compositions, melittin was shown to interact, although not in the same manner, with both negatively-charged and zwitterionic phospholipids. Melittin carries a net charge of +6, and therefore binds better to negatively-charged than to zwitterionic membranes. This has been demonstrated in studies of melittin binding to phosphatidylserine (Dufourcq & Faucon, 1977), cardiolipin (Batenburg et al., 1987a−c), phosphatidylglycerol (Batenburg et al., 1987a−c), phosphatidylcholine/phosphatidylethanolamine (Batenburg et al., 1988), and phosphatidylcholine/phosphatidylglycerol (Beschiaschvili & Seelig, 1990) vesicles. Before binding to membranes, melittin is present in an aqueous solution, and its conformation is determined by a balance of two forces: (i) repulsive forces between positive charges of the monomers, which favor a monomeric form with an extended unfolded state; these repulsive forces can be reduced in the presence of anions or salts; (ii) the opposing forces which favor the formation of helical tetrameres. These forces consist mainly of hydrophobic interactions between the hydrophobic surfaces of the helices (Hagihara et al., 1992). When bound to PC/PS vesicles, the positive charges of melittin are partially neutralized by the negative charges of the phospholipid headgroups, and therefore melittin favors the helical state. This allows the hydrophobic interactions between the nonpolar amino acids located at the hydrophobic surface of the helix and the phospholipid hydrocarbon layer. However, with the zwitterionic PC phospholipids, the rate limiting step appears to be the partial penetration of the peptide into the hydrophobic region of the bilayers (Sekharam et al., 1991), which is probably driven by the intrinsic hydrophobic forces that manifest themselves by forming an α-helical structure. In contrast to native melittin, which bound strongly to both negatively-charged and zwitterionic phospholipids, [D]-$V^{5,8}$,I^{17},K^{21}-melittin bound only to nega-

tively-charged phospholipids (PC/PS) (Figure 5). Thus, electrostatic interactions appear to play an important role in the initial binding of the diastereomers to PC/PS membranes. The disruption of the α-helical structure of melittin, which prevents manifestation of hydrophobic forces, is probably responsible for the inability of [D]-$V^{5,8}$,I^{17},K^{21}-melittin to bind zwitterionic phospholipids. The inability of [D]-$V^{5,8}$,I^{17},K^{21}-melittin to bind to zwitterionic phospholipids can explain therefore why the peptide could not permeate PC vesicles, as determined in the diffusion potential experiments (Figure 4). Interestingly, despite the disruption of its α-helical structure, the mode of interaction of [D]-$V^{5,8}$,I^{17},K^{21}-melittin with PC/PS vesicles is similar to that of native melittin. Both exhibited similar partition coefficients with negative cooperativity (Figure 5B), had the same potency for dissipating diffusion potentials (Figure 4B), and penetrated with the same level into the hydrophobic core of PC/PS vesicles, as seen in the tryptophan quenching experiments using brominated phospholipids (Figure 6). These findings further emphasize that the α-helical structure is not a prerequisite for binding to negatively- charged phospholipid membranes and that electrostatic interactions have an important role in the binding process. Therefore, the higher antibacterial activity of [D]-$V^{5,8}$,I^{17},K^{21}-melittin compared to [D]-$V^{5,8}$,I^{17},K^{21}-melittin-COOH is probably related to the higher net positive charge of the former, rather than the negligible increase in its α-helical structure in comparison to [D]-$V^{5,8}$,I^{17},K^{21}-melittin-COOH. An increase in antibacterial activity due to the addition of positive charges has been demonstrated with other linear lytic peptides as well (Bessalle et al., 1992; Oren & Shai, 1996).

The antibacterial peptide magainin is a nonhemolytic peptide, while melittin and pardaxin are hemolytic. In contrast to melittin and pardaxin, when the α-helical structure of magainin was disrupted by the introduction of a single D-amino acid, the resulting diastereomer completely lost its antibacterial activity (Chen et al., 1988), even though the diastereomer has a net positive charge similar to that of melittin. Nevertheless, magainin has a low affinity and permeating activity for PC vesicles compared to PC/PS vesicles, similarly to properties of other naturally occurring antibacterial peptides studied so far and the diastereomers of melittin and pardaxin**.** An optimal balance may already exist between the α-helical structure, hydrophobicity, and net positive charge of native magainin, which allows selection between the two types of vesicles. Therefore, any change in one of these properties might cause a loss in magainin's antibacterial activity. The relevance of these findings to the biological target membranes of the antibacterial peptides has been attributed to the fact that the surface of bacteria contains lipopolysaccharides (LPS, in Gram-negative bacteria) and polysaccharides (teichoic acids, in Gram-positive bacteria), and their membranes contain phosphatidylglycerol (PG), all of which are acidic, while normal mammalian cells (e.g., erythrocytes) express the predominantly zwitterionic phospholipid PC on their outer leaflet.

Studies on the orientation of melittin bound to phospholipid membranes revealed that melittin is absorbed onto the surface of fully hydrated phospholipid membranes (Altenbach et al., 1989; Altenbach & Hubbell, 1988; Brauner et al., 1987; Dempsey & Butler, 1992; Frey & Tamm, 1991). However, melittin adopts a transmembrane orientation when bound to oriented dry phospholipid membranes (Frey & Tamm, 1991; Jhon & Jahnig, 1991) or if applied with a transmembrane potential (Kempf et al., 1982; Schwarz et al., 1992; Tosteson et al., 1990; Tosteson & Tosteson, 1981). We found that, with both melittin and [D]-$V^{5,8}$,I^{17},K^{21}-melittin, the largest quenching of tryptophan fluorescence occurred with 6.7-Br-PC/PS. These results suggest that, [D]-$V^{5,8}$,I^{17},K^{21}-melittin, like melittin in fully hydrated phospholipid membranes, becomes located parallel to the bilayer surface.

Three fundamentally distinct hypotheses can explain the cytolytic activity of melittin. According to one hypothesis, perturbation of the membrane bilayer, in which the peptide acts as a sort of mechanical "wedge" between lipid molecules, results in the structural disruption of the opposed membrane leaflets (Dawson et al., 1978; Vogel et al., 1983). In another hypothesis, cytotoxicity is caused by the peptide increasing the curvature of the bilayer (Batenburg & de Kruijff, 1988). Alternatively, formation of transmembrane pores in lipid bilayers by the assembly of several monomers via a "barrel-stave" mechanism is responsible for the cytolytic activity of melittin (DeGrado et al., 1982; Tosteson & Tosteson, 1981; Vogel & Jahnig, 1986). According to the latter hypothesis, transmembrane amphipathic α-helices form bundles in which outwardly-directed hydrophobic surfaces interact with the lipid constituents of the membrane, while inwardly-facing hydrophilic surfaces produce a pore. All of these three proposed mechanisms were also proposed to require that lipid-bound melittin assume an α-helical structure. However, our results with melittin diastereomers indicate that α-helical structure is not required for melittin's permeation of negatively-charged membranes. Therefore, the diastereomers cannot form transmembrane pores, but rather bind onto the surface of the membrane (based on the tryptophan quenching experiments, Figure 6), cover the membrane in a "carpet-like" manner, and dissolve it like a detergent. The four steps possibly involved in this model are: (i) preferential binding of peptide monomers to the negatively-charged phospholipids (Figure 5), (ii) laying of the monomers on the surface of the membrane (Figure 6) such that the positive charges of the basic amino acids interact with the negatively charged phospholipid headgroups or water molecules, (iii) reorganization of the molecule leading to reorientation of the hydrophobic residues toward the hydrophobic core of the membrane, and (iv) disintegrating the membrane by disrupting the lipid packing in the bilayer structure (Figures 3 and 4).

Indeed, according to the dissipation of diffusion potential experiments, the maximal membrane- permeating activity of [D]-$V^{5,8}$,I^{17},K^{21}-melittin occurs at a lipid:peptide molar ratio of ∼22:1 (Figure 4). Under these conditions, ∼80% of the peptide is bound to the membrane (calculated from the binding isotherm, Figure 5). Assuming that the peptide binds only to the outer surface (∼60% of total lipid), the lipid: bound peptide molar ratio is ∼10:1. Taking a surface area of 70 $Å^2$ for each phospholipid molecule, the area available for each [D]-$V^{5,8}$,I^{17},K^{21}-melittin monomer is ∼700 $Å^2$. The surface area of a 31 amino acids long α-helical peptide is ∼520 $Å^2$ (Steiner et al., 1988). [D]-$V^{5,8}$,I^{17},K^{21}-Melittin is not an α-helix and probably is more extended than an ideal α-helical peptide. It is reasonable to assume, therefore, that this amount of bound peptide monomers is sufficient to form a monolayer that completely covers the surface of the vesicles. However, it is not unlikely that the diastereomer

also assumes some compact (nonhelical) conformation when bound to negatively-charged PC/PS membranes in order to bury its apolar residues. Since Figure 6 shows that the peptide stays on only one side of the membrane, this would seem to fulfill the first hypothesis of a "wedge" causing an asymmetrical expansion of the outer leaflet. This would also seem to fulfill the second hypothesis, in which melittin causes a localized increase in membrane curvature, thus suggesting that an α-helical structure is not necessary for the two later mechanisms.

The results presented here, together with those obtained with the diastereomers of pardaxin, suggest a new strategy for designing antibacterial peptides that should have some advantages. First, the peptides should lack the diverse pathological and pharmacological effects induced by α-helical lytic cytolysins. For example, staphylococcus δ-toxin, the antibacterial peptide alamethicin, cobra direct lytic factor, and pardaxin exert several histopathological effects on various cells due to pore formation and activation of the arachidonic acid cascade. However, diastereomers of pardaxin did not exert these activities (Shai & Oren, 1996). Furthermore, many amphipathic α-helical peptides bind to calmodulin to elicit several cell responses, and even all D-amino acid α-helices including melittin are endowed with similar activity (Fisher et al., 1994). Diastereomers with disrupted α-helical structure should not bind to calmodulin. Second, local D-amino acid substitution should enable controlled clearance of the antibacterial peptides by proteolytic enzymes, rather than the total protection acquired by complete D-amino substitution (Wade et al., 1990; Bessalle et al., 1990). Total resistance of a lytic peptide to degradation might be disadvantageous for therapeutic use. Furthermore, the antigenicity of short fragments containing D,L-amino acids is dramatically diffferent than that of their entire L- or D-amino acid parent molecules (Benkirane et al., 1993). Third, total inhibition of bacterial growth induced by the diastereomrs is associated with total lysis of the bacterial wall, as shown by electron microscope (Figure 3). Therefore, bacteria might not easily develop resistance to drugs that employ such a destructive mechanism.

In summary, the results obtained with the diastereomers of pardaxin and melittin indicate that neither a specific sequence, length, nor position of D-amino acids is prerequisite for a polypeptide to acquire antibacterial activity. However, these factors seem to be more crucial for cytotoxicity toward mammalian cells. Despite the fact that the biological activities and the mode of action of pardaxin and melittin are not the same, their diastereomers act on model membranes and bacteria in a similar fashion. Therefore, we suggest that modulating both the hydrophobicity and net positive charge of diastereomers of linear cytotoxic polypeptide may be sufficient to design potent antibacterial polypeptides for the treatment of infectious diseases.

REFERENCES

Altenbach, C., & Hubbell, W. L. (1988) *Proteins 3*, 230−242.

Altenbach, C., Froncisz, W., Hyde, J. S., & Hubbell, W. L. (1989) *Biophys. J. 56*, 1183−1191.

Anderson, D., Terwilliger, T. C., Wickner, W., & Eisenberg, D. (1980) *J. Biol. Chem. 255*, 2578−2582.

Bartlett, G. R. (1959) *J. Biol. Chem. 234*, 466−468.

Batenburg, A. M., & de Kruijff, B. (1988) *Biosci. Rep. 8*, 299−307.

Batenburg, A. M., Hibbeln, J. C., & de Kruijff, B. (1987a) *Biochim. Biophys. Acta 903*, 155−165.

Batenburg, A. M., Hibbeln, J. C., Verkleij, A. J., & de Kruijff, B. (1987b) *Biochim. Biophys. Acta 903*, 142−154.

Batenburg, A. M., van Esch, J., Leunissen, B. J., Verkleij, A. J., & de Kruijff, B. (1987c) *FEBS Lett. 223*, 148−154.

Batenburg, A. M., van Esch, J., & de Kruijff, B. (1988) *Biochemistry 27*, 2324−2331.

Bazzo, R., Tappin, M. J., Pastore, A., Harvey, T. S., Carver, J. A., & Campbell, I. D. (1988) *Eur. J. Biochem. 173*, 139−146.

Benkirane, N., Friede, M., Guichard, G., Briand, J. P., Van, R. M., & Muller, S. (1993) *J. Biol. Chem. 268*, 26279−26285.

Beschiaschvili, G., & Seelig, J. (1990) *Biochemistry 29*, 52−58.

Bessalle, R., Kapitkovsky, A., Gorea, A., Shalit, I., & Fridkin, M. (1990) *FEBS Lett. 274*, 1−2.

Bessalle, R., Haas, H., Goria, A., Shalit, I., & Fridkin, M. (1992) *Antimicrob. Agents Chemother. 36*, 313−317.

Blondelle, S. E., & Houghten, R. A. (1991) *Biochemistry 30*, 4671−4678.

Bolen, E. J., & Holloway, P. W. (1990) *Biochemistry 29*, 9638−9643.

Boman, H. G. (1995) *Annu. Rev. Immunol. 13*, 61−92.

Brauner, J. W., Mendelsohn, R., & Prendergast, F. G. (1987) *Biochemistry 26*, 8151−8158.

Chen, H. C., Brown, J. H., Morell, J. L., & Huang, C. M. (1988) *FEBS Lett. 236*, 462−466.

Dawson, C. R., Drake, A. F., Helliwell, J., & Hider, R. C. (1978) *Biochim. Biophys. Acta 510*, 75−86.

DeGrado, W. F., Musso, G. F., Lieber, M., Kaiser, E. T., & Kezdy, F. J. (1982) *Biophys. J. 37*, 329−338.

De Kroon, A. I., Soekarjo, M. W., De Gier, J., & De Kruijff, B. (1990) *Biochemistry 29*, 8229−8240.

Dempsey, C. E. (1990) *Biochim. Biophys. Acta 1031*, 143−161.

Dempsey, C. E., & Butler, G. S. (1992) *Biochemistry 31*, 11973−11977.

Dhople, V. M., & Nagaraj, R. (1993) *Biosci. Rep. 13*, 245−250.

Dufourcq, J., & Faucon, J. F. (1977) *Biochim. Biophys. Acta 467*, 1−11.

Fisher, P. J., Prendergast, F. G., Ehrhardt, M. R., Urbauer, J. L., Wand, A. J., Sedarous, S. S., McCormick, D. J., & Buckley, P. J. (1994) *Nature 368*, 651−653.

Frey, S., & Tamm, L. K. (1991) *Biophys. J. 60*, 922−930.

Greenfield, N., & Fasman, G. D. (1969) *Biochemistry 8*, 4108−4116.

Habermann, E., & Jentsch, J. (1967) *Hoppe Seyler's Z. Physiol. Chem. 348*, 37−50.

Hagihara, Y., Kataoka, M., Aimoto, S., & Goto, Y. (1992) *Biochemistry 31*, 11908−11914.

Hider, R. C., Khader, F., & Tatham, A. S. (1983) *Biochim. Biophys. Acta 728*, 206−214.

Jhon, E., & Jahnig, F. (1991) *Biophys. J. 60*, 319−328.

Kempf, C., Klausner, R. D., Weinstein, J. N., Van, R. J., Pincus, M., & Blumenthal, R. (1982) *J. Biol. Chem. 257*, 2469−2476.

Kuchinka, E., & Seelig, J. (1989) *Biochemistry 28*, 4216−4221.

Lazarovici, P., Primor, N., & Loew, L. M. (1986) *J. Biol. Chem. 261*, 16704−16713.

Li, Z. Q., Merrifield, R. B., Boman, I. A., & Boman, H. G. (1988) *FEBS Lett. 231*, 299−302.

Loew, L. M., Rosenberg, I., Bridge, M., & Gitler, C. (1983) *Biochemistry 22*, 837−844.

Merrifield, R. B., Vizioli, L. D., & Boman, H. G. (1982) *Biochemistry 21*, 5020−5031.

Mor, A., Nguyen, V. H., Delfour, A., Migliore, S. D., & Nicolas, P. (1991) *Biochemistry 30*, 8824−8830.

Oren, Z., & Shai, Y. (1996) *Eur. J. Biochem. 237*, 303−310.

Papahadjopoulos, D., & Miller, N. (1967) *Biochim. Biophys. Acta 135*, 624−638.

Perez, P. E., Houghten, R. A., & Blondelle, S. E. (1994) *Biochem. J. 299*, 587−591.

Perez, P. E., Houghten, R. A., & Blondelle, S. E. (1995) *J. Biol. Chem. 270*, 1048−1056.

Rapaport, D., & Shai, Y. (1991) *J. Biol. Chem. 266*, 23769−23775.

Rapaport, D., Peled, R., Nir, S., & Shai, Y. (1996) *Biophys. J. 70*, 2502−2512.

Rothemund, S., Beyermann, M., Krause, E., Krause, G., Bienert, M., Hodges, R. S., Sykes, B. D., & S, o. F. (1995) *Biochemistry 34*, 12954−12962.
Schwarz, G., Gerke, H., Rizzo, V., & Stankowski, S. (1987) *Biophys. J. 52*, 685−692.
Schwarz, G., Zong, R. T., & Popescu, T. (1992) *Biochim. Biophys. Acta 1110*, 97−104.
Segrest, J. P., de-Loof, H., Dohlman, J. G., Brouillette, C. G., & Anantharamaiah, G. M. (1990) *Proteins 8*, 103−117.
Sekharam, K. M., Bradrick, T. D., & Georghiou, S. (1991) *Biochim. Biophys. Acta 1063*, 171−174.
Shai, Y., & Oren, Z. (1996) *J. Biol. Chem 271*, 7305−7308.
Shai, Y., Fox, J., Caratsch, C., Shih, Y. L., Edwards, C., & Lazarovici, P. (1988) *FEBS Lett. 242*, 161−166.
Shai, Y., Bach, D., & Yanovsky, A. (1990) *J. Biol. Chem. 265*, 20202−20209.
Shai, Y., Hadari, Y. R., & Finkels, A. (1991) *J. Biol. Chem. 266*, 22346−22354.
Sims, P. J., Waggoner, A. S., Wang, C. H., & Hoffmann, J. R. (1974) *Biochemistry 13*, 3315−3330.
Steiner, H., Hultmark, D., Engstrom, A., Bennich, H., & Boman, H. G. (1981) *Nature 292*, 246−248.
Terwilliger, T. C., & Eisenberg, D. (1982a) *J. Biol. Chem. 257*, 6010−6015.
Terwilliger, T. C., & Eisenberg, D. (1982b) *J. Biol. Chem. 257*, 6016−6022.
Thompson, S. A., Tachibana, K., Nakanishi, K., & Kubota, I. (1986) *Science 233*, 341−343.
Tosteson, M. T., & Tosteson, D. C. (1981) *Biophys. J. 36*, 109−116.
Tosteson, M. T., Alvarez, O., Hubbell, W., Bieganski, R. M., Attenbach, C., Caporales, L. H., Levy, J. J., Nutt, R. F., Rosenblatt, M., & Tosteson, D. C. (1990) *Biophys. J. 58*, 1367−1375.
Vogel, H., & Jahnig, F. (1986) *Biophys. J. 50*, 573−582.
Vogel, H., Jahnig, F., Hoffmann, V., & Stumpel, J. (1983) *Biochim. Biophys. Acta 733*, 201−209.
Wade, D., Boman, A., Wahlin, B., Drain, C. M., Andreu, D., Boman, H. G., & Merrifield, R. B. (1990) *Proc. Natl. Acad. Sci. U.S.A. 87*, 4761−4765.
Wade, D., Andreu, D., Mitchell, S. A., Silveira, A. M., Boman, A., Boman, H. G., & Merrifield, R. B. (1992) *Int. J. Pept. Protein Res. 40*, 429−436.
Weaver, A. J., Kemple, M. D., Brauner, J. W., Mendelsohn, R., & Prendergast, F. G. (1992) *Biochemistry 31*, 1301−1313.
Wu, C. S., Ikeda, K., & Yang, J. T. (1981) *Biochemistry 20*, 566−570.
Zasloff, M. (1987) *Proc. Natl. Acad. Sci. U.S.A. 84*, 5449−5453.

BI962507L